Canadian Journal of Pure and Applied Sciences
Vol. 1, No. 1, pp. 83-96, 2007

SENRA Academic Publishers, Burnaby, British Columbia
ISSN: 1715-9997

NUMERICAL SOLUTION OF COUPLE STRESS FULL REYNOLDS EQUATION FOR PLANE INCLINED POROUS SLIDER BEARINGS WITH SQUEEZING EFFECT

NB Naduvinamani[1]* and GB Marali[2]
[1] Department of Mathematics, Gulbarga University, Gulbarga-585106, India
[2] Department of Mathematics, B.V.B. College of Engineering and Technology
Hubli-580031, India

ABSTRACT

In this paper a general dynamic Reynolds equation of sliding-squeezing surfaces with couple stress fluids is derived for the assessment of static and dynamic characteristics of porous bearings. The analysis takes into account of transient squeezing action effects and velocity slip at the porous/fluid film interface by using the modified B-J slip boundary conditions. The numerical solution of two-dimensional plane inclined porous slider bearing is illustrated. Using the perturbation technique two Reynolds-type equations governing the steady performance and the perturbed characteristics are obtained. The steady and perturbed characteristics are then numerically calculated by using finite-difference technique. From the numerical results computed it is observed that there exists a critical value for the profile parameter at which the steady-state load and dynamic stiffness coefficients attains maximum. Further it is found that this critical value of the profile parameter is a function of permeability parameter. The effects of couple stresses provide an improved performance for both steady-state, dynamic stiffness and damping characteristics. This effect is more accentuated for the porous bearings with larger values of aspect ratio.

Keywords: Numerical solution, full reynolds equation, steady-state, porous, slider bearing, couple stress.

INTRODUCTION

Porous bearings have the features of simple structure and low cost. Porous bearings are used where non-porous bearings are impracticable owing to lack of space or inaccessibility for lubrication. The application of porous bearings in mounting horsepower motors include vacuum cleaners, coffee grinders, hair driers, saving machines, sewing machines, water pumps, record players, tape recorders, generators and distributors. Kumar (1980), Murti (1974a), Sanni and Ayomidele (1991), Srinivasan (1977) and Verma *et al*. (1978) have analyzed the porous slider bearings by using Darcy's equation to model the flow of Newtonian lubricant in the porous matrix. All these studies assume the lubricant to be Newtonian fluid. In most of the modern equipments, the increasing velocities of rotating units, higher impact loads acting on supports and the application of new structural materials are adopted. The performance of the friction unit of a machine can be improved by the application of new bearing materials. The cintered ceramets and also the materials manufactured by the methods of gas-thermal spraying are such materials. The bearings with these materials operate with less noise as compared to the costly non-ferrous metals Akhverdiev *et al*. (2000). The hydrodynamic lubrication theory of porous bearings was first studied by Morgan and Cameron (1957). The squeeze film behavior in porous circular disc was studied by Murti (1974b). The centrifugal effects in hydrostatic porous thrust bearings studied by Gupta and Kapur (1979). There have been several studies of porous bearings such as porous slider bearings by Uma (1977) and porous journal bearings by Prakash and Vij (1974), porous squeeze films by Wu (1972). All these studies on porous bearings are confined to Newtonian lubricants.

The use of non-Newtonian fluids as lubricant is of growing interest in the recent years. Most of these modern lubricating oils contain high molecular weight polymer additives as a kind of viscosity improver. These additives which are polymers or co-polymers are added to the base oils in order to prevent the viscosity variation with temperature, these are characterized by long chains in which the length of polymer chain may be a million times the diameter of water molecule Lahmar (2005) and these are classified into hydrodynamic co-polymers and polymethacarylates. The experimental study of Robin (1978) revealed that the use of oils with a higher concentration of viscosity index additives having low molecular weight is more advantageous than the use of lower concentration of additives with higher molecular weight.

The conventional study of hydrodynamic bearings assumes that, the lubricant as a Newtonian fluid. The classical Newtonian continuum mechanics of fluids neglects the size of fluid particles. Hence several micro-continuum theories have been proposed by Ariman *et al*. (1973) and Ariman *et al*. (1974) to account for the size effects of fluid particles, because Stokes (1966) micro-continuum theory for the couple stress fluids is the generalization of classical Newtonian fluid theory and it accounts for the polar effects such as the couple stresses, body couples and asymmetric tensors. Several investigators used Stokes micro-continuum theory for couple stress fluids for the study of several bearing

*Corresponding author: E-mail: naduvinamaninb@yahoo.co.in

systems Bujurke *et al*. (2005), Nuduvinamani *et al*. (2001a), Naduvinamani *et al*. (2002), Naduvinamani *et al*. (2004), Ramanaiah and Priti Sarkar (1978) and Ramanaiah (1979) have been reported several advantages over the Newtonian lubricants. So for no attempt has been made to study the static and dynamic characteristics of porous inclined slider bearings with couple stress fluids by including the squeezing action of the bearing surfaces. Hence in this paper an attempt has been made to derive the dynamic modified Reynolds type equation for the couple stress fluids for porous slider bearings with squeezing action of the surfaces and detailed numerical analysis is presented for the two dimensional porous slider bearings.

MATHODS

The basic equations derived by Stokes (1966) for the motion of an incompressible couple stress fluid, in the absence of body forces and body moments are

$$\rho\frac{D\vec{q}}{Dt} = -\nabla p + \mu\nabla^2\vec{q} - \eta\nabla^4\vec{q} \tag{2.1}$$

$$\nabla.\vec{q} = 0 \tag{2.2}$$

where ρ is the density, $\vec{q}$ is the velocity vector, p is the pressure, μ is the Newtonian shear viscosity and η is a material constant accounting for the couple stress property. The ratio $\left(\frac{\eta}{\mu}\right)$ has the dimensions of the length squared and hence the dimension of $\sqrt{\frac{\eta}{\mu}}$ characterizes the material length of the couple stress fluid.

A geometry for the physical configuration of the problem under consideration is shown in the Fig.1. It consists of porous slider with sliding velocity U including the effect of the squeezing action $\frac{\partial h}{\partial t}$, $h_1(t)$ is the inlet film thickness and the outlet film thickness is $h_0(t)$. The porous region is assumed to be homogenous and isotropic and the lubricant is incompressible couple stress fluid. Under the usual assumptions of the hydrodynamic lubrication applicable for thin films Pinkus and Sternlicht (1961), the equations of motion (2.1) and (2.2) take the form;

$$\frac{\partial p}{\partial x} = \mu\frac{\partial^2 u}{\partial y^2} - \eta\frac{\partial^4 u}{\partial y^4} \tag{2.3}$$

$$\frac{\partial p}{\partial z} = \mu\frac{\partial^2 w}{\partial y^2} - \eta\frac{\partial^4 w}{\partial y^4} \tag{2.4}$$

$$\frac{\partial p}{\partial y} = 0 \tag{2.5}$$

$$\frac{\partial u}{\partial x} + \frac{\partial v}{\partial y} + \frac{\partial w}{\partial z} = 0 \tag{2.6}$$

The relevant boundary conditions for velocity components are

(i) At the upper solid surface ($y = h$)

$u = w = 0$ (no slip) (2.7a)

$$v = \frac{\partial h}{\partial t} \quad \text{(squeezing velocity)} \tag{2.7b}$$

$$\frac{\partial^2 u}{\partial y^2} = \frac{\partial^2 w}{\partial y^2} = 0 \quad \text{(vanishing of couple stresses)} \tag{2.7c}$$

(ii) At the fluid porous interface ($y = 0$)

$$u = U + \frac{1}{s}\frac{\partial u}{\partial y} \tag{2.8a}$$

$v = -v_1$ (continuity of vertical component) (2.8b)

$$w = \frac{1}{s}\frac{\partial w}{\partial y} \quad \text{(modified B-J slip condition)} \tag{2.8c}$$

$$\frac{\partial^2 u}{\partial y^2} = \frac{\partial^2 w}{\partial y^2} = 0 \text{ (vanishing of couple stresses)} \tag{2.8d}$$

where $s = \frac{\alpha}{\sqrt{k}}$ is the slip parameter, k is the permeability of the porous material, α is a non-dimensional slip coefficient which depends on the characteristics of the porous material.

The solution of Eqn. (2.3) and Eqn. (2.4) subject to boundary conditions (2.7a), (2.7c), (2.8a), (2.8c) and (2.8d) is given by

$$u = \frac{1}{2\mu}\frac{\partial p}{\partial x}\left[(y-h)\left\{y + h\xi - 2l\xi.\tanh\left(\frac{h}{2l}\right)\right\} + 2l^2\left\{1 - \frac{\cosh\left(\frac{2y-h}{2l}\right)}{\cosh\left(\frac{h}{2l}\right)}\right\}\right] - Us(y-h)\xi \tag{2.9}$$

$$w = \frac{1}{2\mu}\frac{\partial p}{\partial z}\left[(y-h)\left\{y + h\xi - 2l\xi.\tanh\left(\frac{h}{2l}\right)\right\} + 2l^2\left\{1 - \frac{\cosh\left(\frac{2y-h}{2l}\right)}{\cosh\left(\frac{h}{2l}\right)}\right\}\right] \tag{2.10}$$

where $l = \sqrt{\frac{\eta}{\mu}}$ and $\xi = \frac{l}{l+hs}$

Integration of continuity equation (2.6) with respect to y over the film thickness gives;

$$-\int_{y=0}^{h}\frac{\partial v}{\partial y}dy = \int_{y=0}^{h}\left(\frac{\partial u}{\partial x} + \frac{\partial w}{\partial z}\right)dy \tag{2.11}$$

By replacing the velocity components u and w with their expressions given in Eqn. (2.9) and Eqn. (2.10), and also using the boundary conditions (2.7b) and (2.8b), the Eqn. (2.11) gives the modified Reynolds type equation in the form

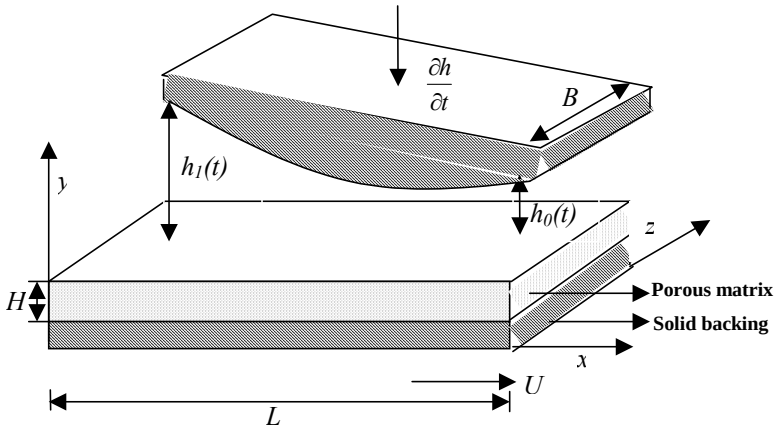

Fig.1. Physical geometry of porous slider bearing

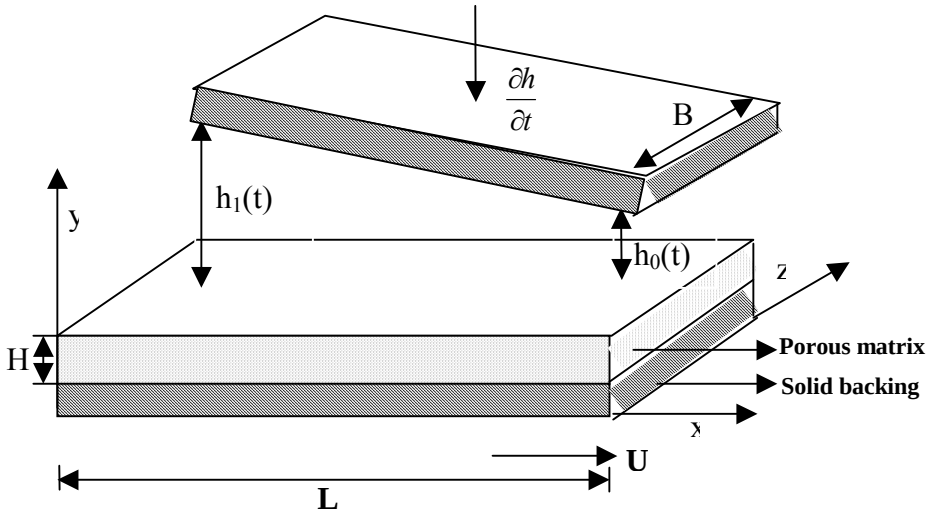

Fig.2. Physical geometry of porous plane inclined slider bearing

$$\frac{\partial}{\partial x}\left[f(h,l,\xi)\frac{\partial p}{\partial x}\right]+\frac{\partial}{\partial z}\left[f(h,l,\xi)\frac{\partial p}{\partial z}\right]=12\mu\frac{\partial h}{\partial t}+6\mu Us\frac{\partial h}{\partial x}+12\mu\left(v_1\right)_{y=0} \quad (2.12)$$

where

$$f(h,l,\xi) = h^3\left(1+3\xi\right)-6h^2l\xi\tanh\left(\frac{h}{2l}\right)-12l^2h+24l^3\tanh\left(\frac{h}{2l}\right) \quad (2.13)$$

The flow of couple stress fluid in a porous matrix is governed by the modified form of Darcy law which accounts for polar effects given by Naduvinamani *et al*. (2001b)

$$u_1 = \frac{-k}{\mu(1-\beta)}\frac{\partial p^*}{\partial x} \quad (2.14)$$

$$v_1 = \frac{-k}{\mu(1-\beta)}\frac{\partial p^*}{\partial y} \quad (2.15)$$

$$w_1 = \frac{-k}{\mu(1-\beta)}\frac{\partial p^*}{\partial z} \quad (2.16)$$

where u_1, v_1, w_1 are modified Darcy velocity components along *x, y, z* directions, respectively, p^* is the pressure in the porous region, $\beta=(\eta/\mu)/k$. The parameter represents the ratio of microstructure size to the pore size. For the flow of couple stress fluid in the porous matrix $\beta << 1$. Due to continuity of fluid in the porous matrix, the pressure p^* satisfies the Laplace equation

$$\frac{\partial^2 p^*}{\partial x^2}+\frac{\partial^2 p^*}{\partial y^2}+\frac{\partial^2 p^*}{\partial z^2}=0\,. \quad (2.17)$$

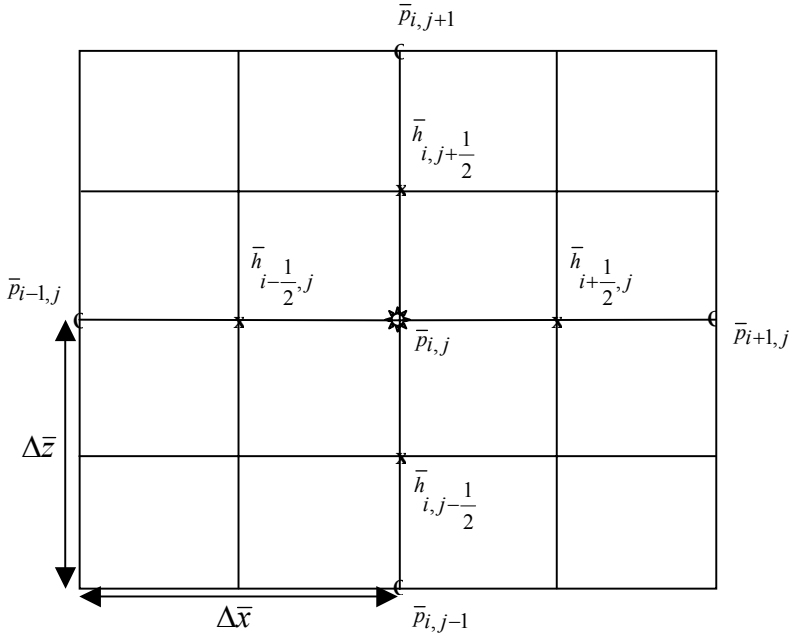

Fig.3. Grid point notation for film domain

Integrating with respect to y over the porous layer thickness H and using the boundary condition of solid backing $\left(\frac{\partial p^*}{\partial y}=0\right)$ at $y = -H$, we obtain

$$\left(\frac{\partial p^*}{\partial y}\right)_{y=0} = -\int_{-H}^{0}\left(\frac{\partial^2 p^*}{\partial x^2}+\frac{\partial^2 p^*}{\partial z^2}\right)dy \tag{2.18}$$

Assuming the porous layer thickness H to be very small and using the continuity condition of pressure ($p = p^*$) at the porous interface ($y = 0$), Eqn. (2.18) reduces to

$$\left(\frac{\partial p^*}{\partial y}\right)_{y=0} = -H\left(\frac{\partial^2 p^*}{\partial x^2}+\frac{\partial^2 p^*}{\partial z^2}\right) \tag{2.19}$$

then the velocity component v_1 at the interface ($y = 0$) is given by

$$(v_1)_{y=0} = -\frac{kH}{\mu(1-\beta)}\left(\frac{\partial^2 p}{\partial x^2}+\frac{\partial^2 p}{\partial z^2}\right) \tag{2.20}$$

Substituting Eqn. (2.20) in Eqn. (2.12), the Dynamic Reynolds equation is obtained in the form

$$\frac{\partial}{\partial x}\left[\left\{f(h,l,\xi)+\frac{12kH}{(1-\beta)}\right\}\frac{\partial p}{\partial x}\right]+\frac{\partial}{\partial z}\left[\left\{f(h,l,\xi)+\frac{12kH}{(1-\beta)}\right\}\frac{\partial p}{\partial z}\right] = 12\,\mu\frac{\partial h}{\partial t}+6U\mu\frac{\partial}{\partial x}(h^2\xi) \tag{2.21}$$

Introducing the non-dimensional quantities ;

$$\bar{h}=\frac{h}{h_{m0}},\ \bar{p}=\frac{ph_{m0}^2}{LU\mu},\ \bar{t}=\frac{Ut}{L},\ \bar{x}=\frac{x}{L},\ \bar{z}=\frac{z}{B},\ \psi=\frac{kH}{h_{m0}^3},\ \bar{s}=sh_{m0},\ \bar{l}=\frac{l}{h_{m0}} \tag{2.22}$$

After introducing the non-dimensional quantities, the dynamic Reynolds equation for the porous slider bearings can be expressed in a non-dimensional form as

$$\frac{\partial}{\partial\bar{x}}\left[\left\{\bar{f}(\bar{h},\bar{l},\bar{\xi})+\frac{12\psi}{(1-\beta)}\right\}\frac{\partial\bar{p}}{\partial\bar{x}}\right]+\frac{1}{\delta^2}\left[\left\{\bar{f}(\bar{h},\bar{l},\bar{\xi})+\frac{12\psi}{(1-\beta)}\right\}\frac{\partial^2\bar{p}}{\partial\bar{z}^2}\right] = 12\frac{\partial\bar{h}}{\partial\bar{t}}+6\frac{\partial}{\partial\bar{x}}\left[\bar{h}\left(1+\frac{\bar{s}_1}{\bar{h}}\right)^{-1}\right] \tag{2.23}$$

Where

$$\bar{f}(\bar{h},\bar{l},\bar{\xi}) = \bar{h}^3(1+3\bar{\xi})-6\bar{h}^2\bar{l}\bar{\xi}\tanh\left(\frac{\bar{h}}{2\bar{l}}\right)-12\bar{l}^2\bar{h}+24\bar{l}^3\tanh\left(\frac{\bar{h}}{2\bar{l}}\right) \tag{2.24}$$

and $\bar{s}_1 = 1/\bar{s}$.

The last term in the Eqn. (2.23) is approximated with $(\bar{h}-\bar{s}_1)$ as $\left(\bar{s}_1/\bar{h}\right)$ is small.

In the limiting case $\psi \to 0$ and $\bar{s}_1 \to 0$ Eqn. (2.23) reduces to the solid case studied by Lin *et al*. (2003).

POROUS PLANE INCLINED SLIDER BEARING

A schematic diagram of the porous plane inclined slider bearing with squeezing action is shown in the fig. 2.

To study the static and dynamic characteristics of the porous plane inclined slider bearing, the film thickness is separated into two parts: the minimum film thickness $h_m(t)$ and the slider profile function $h_s(x)$

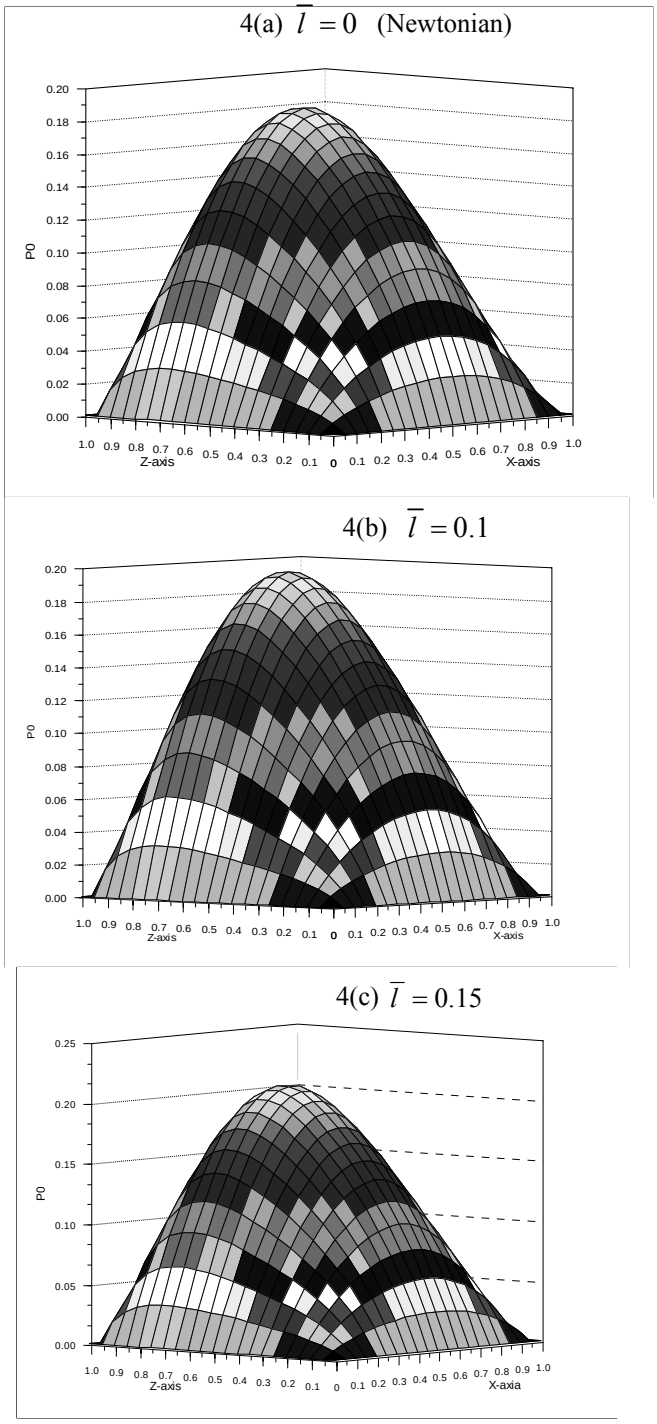

Fig. 4. Non-dimensional steady-state pressure P_0 for different values of $\bar{l}$ with $\psi = 0.01, \lambda = 0.75$, $\beta = 0.3$ and $\delta = 1.5$

$$h(x,t) = h_m(t) + h_s(x) = h_m(t) + a\left(1 - \frac{x}{L}\right)$$

where $a = h_1(t) - h_0(t)$

and its non-dimensional form is

$$\bar{h}(\bar{x},\bar{t}) = \bar{h}_m(\bar{t}) + \bar{h}_s(\bar{x}) = \bar{h}_m(\bar{t}) + \lambda(1-\bar{x}) \qquad (3.1)$$

where $\lambda\left(=\frac{a}{h_{m0}}\right)$ is the slider-profile parameter

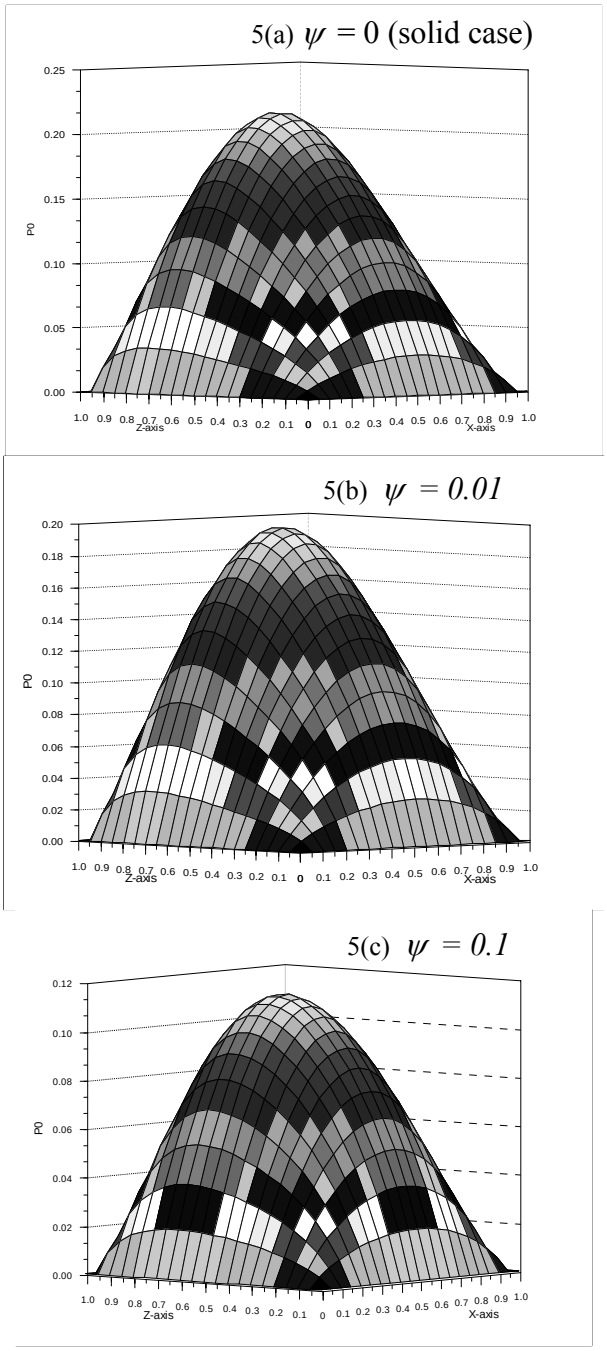

Fig. 5. Non-dimensional steady-state pressure P_0 for different values of ψ with $\bar{l} = 0.1$, $\lambda = 0.75$, $\beta = 0.3$ and $\delta = 1.5$

The steady and dynamic characteristics of the porous bearings are obtained by using the perturbations in h_{m0}.

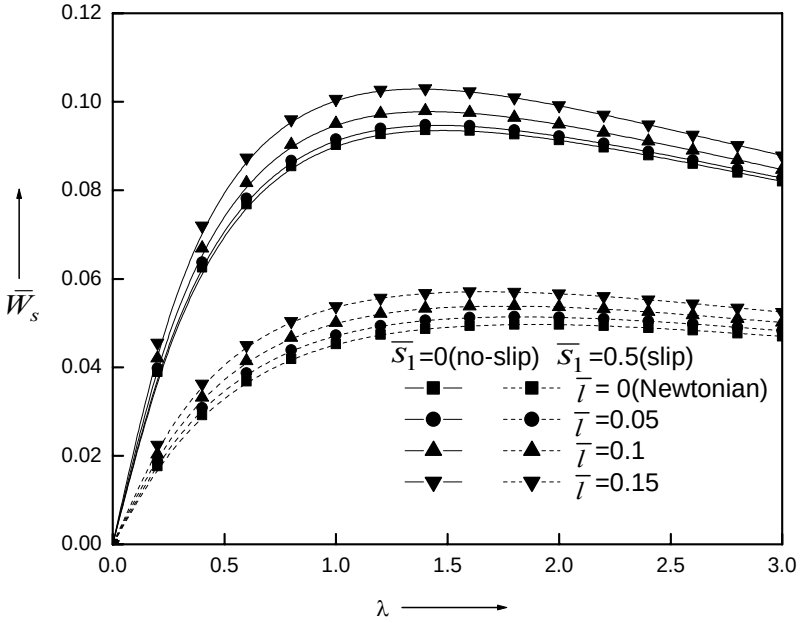

Fig.6 Variation of non-dimensional steady load-carrying capacity $\overline{W}_s$ with profile parameter λ for δ = 1.5, ψ = 0.01, β= 0.3

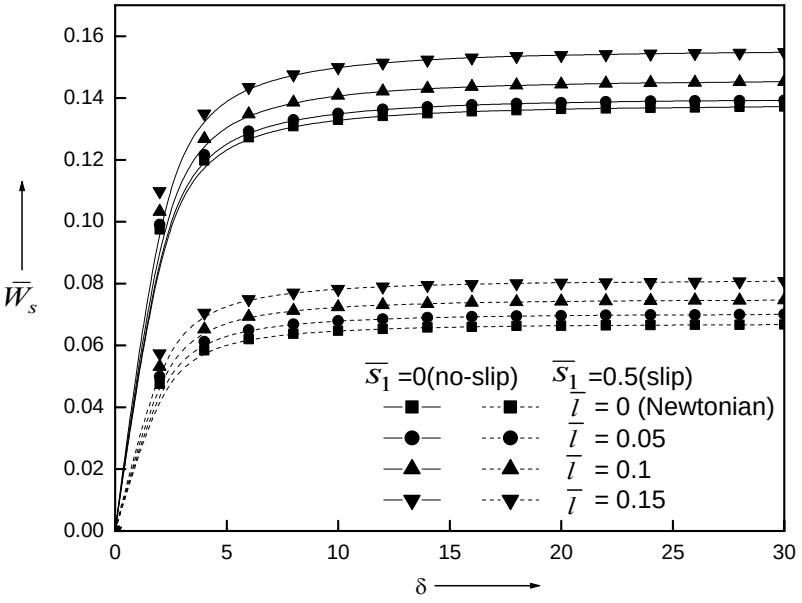

Fig.7 Variation of non-dimensional steady load-carrying capacity $\overline{W}_s$ with aspect ratio δ for λ= 0.75, ψ = 0.01, β= 0.3

The minimum film thickness and the local film pressure are assumed to be of the form

$$\overline{h}_m = 1 + \varepsilon e^{i\overline{t}}, \quad \overline{p} = \overline{p}_0 + \overline{p}_1 \varepsilon e^{i\overline{t}} \tag{3.2}$$

where ε is the perturbation amplitude and is assumed to be small and $i = \sqrt{-1}$

Substituting into the dynamic Reynolds-type equation (2.23) and neglecting the higher order terms of ε, the two Reynolds-type equations responsible for both steady-state pressure and the perturbed film pressure obtained are

$$\frac{\partial}{\partial\bar{x}}\left[\left\{\bar{f}_0(\bar{h}_s,\bar{l},\bar{s}_1)+\frac{12\psi}{(1-\beta)}\right\}\frac{\partial\bar{p}_0}{\partial\bar{x}}\right]+\frac{1}{\delta^2}\left\{\bar{f}_0(\bar{h}_s,\bar{l},\bar{s}_1)+\frac{12\psi}{(1-\beta)}\right\}\frac{\partial^2\bar{p}_0}{\partial\bar{x}^2}=-6\lambda \tag{3.3}$$

$$\frac{\partial}{\partial\bar{x}}\left[\bar{f}_1(\bar{h}_s,\bar{l},\bar{s}_1)\frac{\partial\bar{p}_0}{\partial\bar{x}}+\left\{\bar{f}_0(\bar{h}_s,\bar{l},\bar{s}_1)+\frac{12\psi}{(1-\beta)}\right\}\frac{\partial\bar{p}_1}{\partial\bar{x}}\right]+ \tag{3.4}$$

$$\frac{1}{\delta^2}\left[\bar{f}_1(\bar{h}_s,\bar{l},\bar{s}_1)\frac{\partial^2\bar{p}_0}{\partial\bar{z}^2}+\left\{\bar{f}_0(\bar{h}_s,\bar{l},\bar{s}_1)+\frac{12\psi}{(1-\beta)}\right\}\frac{\partial^2\bar{p}_1}{\partial\bar{z}^2}\right]=12i$$

where

$$\bar{f}_0(\bar{h}_s,\bar{l},\bar{s}_1)=(1+\bar{h}_s)^3+3\bar{s}_1(1+\bar{h}_s)^2-12\bar{l}^2(1+\bar{h}_s) \tag{3.5}$$
$$-6\bar{l}\,\bar{s}_1(1+\bar{h}_s)\tanh\left(\frac{1+\bar{h}_s}{2\bar{l}}\right)+24\bar{l}^3\tanh\left(\frac{1+\bar{h}_s}{2\bar{l}}\right)$$

$$\bar{f}_1(\bar{h}_s,\bar{l},\bar{s}_1)=3(1+\bar{h}_s)^2+6\bar{s}_1(1+\bar{h}_s)-12\bar{l}^2-6\bar{l}\,\bar{s}_1(1+\bar{h}_s)\tanh\left(\frac{1+\bar{h}_s}{2\bar{l}}\right) \tag{3.6}$$
$$+\left\{12\bar{l}^2-3(1+\bar{h}_s)\bar{s}_1\right\}\sec^2h\left(\frac{1+\bar{h}_s}{2\bar{l}}\right)$$

The boundary conditions for the steady and perturbed film pressure are

$$\bar{p}_0=0 \quad at\ \bar{x}=0,\ \bar{x}=1,\bar{y}=0,\bar{y}=1 \tag{3.7}$$

$$\bar{p}_1=0 \quad at\ \bar{x}=0,\ \bar{x}=1,\bar{y}=0,\bar{y}=1 \tag{3.8}$$

The modified Reynolds equation will be solved numerically by using a finite difference scheme. Fig.. 3 shows the film domain divided by grid spacing.

In finite increment format, the terms in the Eqn. (3.3) and Eqn. (3.4) can be expressed as

$$\frac{\partial}{\partial\bar{x}}\left[\left(\bar{f}_0+\frac{12\psi}{(1-\beta)}\right)\frac{\partial\bar{p}_0}{\partial\bar{x}}\right]=\frac{1}{\Delta\bar{x}}\left[\left(\bar{f}_{0i+\frac{1}{2},j}+\frac{12\psi}{(1-\beta)}\right)\left\{\frac{\bar{p}_{0i+1,j}-\bar{p}_{0i,j}}{\Delta\bar{x}}\right\}-\left(\bar{f}_{0i-\frac{1}{2},j}+\frac{12\psi}{(1-\beta)}\right)\left\{\frac{\bar{p}_{0i,j}-\bar{p}_{0i-1,j}}{\Delta\bar{x}}\right\}\right]$$

$$\left(\bar{f}_0+\frac{12\psi}{1-\beta}\right)\frac{\partial^2\bar{p}_0}{\partial\bar{z}^2}=\frac{1}{(\Delta\bar{z})^2}\left(\bar{f}_{0i,j}+\frac{12\psi}{(1-\beta)}\right)\left[\bar{p}_{0i,j+1}-2\bar{p}_{0i,j}+\bar{p}_{0i,j-1}\right]$$

,

$$\frac{\partial}{\partial\bar{x}}\left[\left(\bar{f}_0+\frac{12\psi}{1-\beta}\right)\frac{\partial\bar{p}_1}{\partial\bar{x}}+\bar{f}_1\frac{\partial\bar{p}_0}{\partial\bar{x}}\right]=\frac{1}{\Delta\bar{x}}\left[\left(\bar{f}_{0i+\frac{1}{2},j}+\frac{12\psi}{(1-\beta)}\right)\left\{\frac{\bar{p}_{1i+1,j}-\bar{p}_{1i,j}}{\Delta\bar{x}}\right\}-\left(\bar{f}_{0i-\frac{1}{2},j}+\frac{12\psi}{(1-\beta)}\right)\left\{\frac{\bar{p}_{1i,j}-\bar{p}_{1i-1,j}}{\Delta\bar{x}}\right\}\right]$$
$$+\frac{1}{\Delta\bar{x}}\left[\bar{f}_{1i+\frac{1}{2},j}\left\{\frac{\bar{p}_{0i+1,j}-\bar{p}_{0i,j}}{\Delta\bar{x}}\right\}-\bar{f}_{1i-\frac{1}{2},j}\left\{\frac{\bar{p}_{0i,j}-\bar{p}_{0i-1,j}}{\Delta\bar{x}}\right\}\right]$$

and

$$\left(\bar{f}_0+\frac{12\psi}{1-\beta}\right)\frac{\partial^2\bar{p}_1}{\partial\bar{z}^2}+\bar{f}_1\frac{\partial^2\bar{p}_0}{\partial\bar{z}^2}=\frac{1}{(\Delta\bar{z})^2}\left(\bar{f}_{0i,j}+\frac{12\psi}{(1-\beta)}\right)\left[\bar{p}_{1i,j+1}-2\bar{p}_{1i,j}+\bar{p}_{1i,j-1}\right]$$
$$+\frac{1}{(\Delta\bar{z})^2}\bar{f}_{1i,j}\left[\bar{p}_{0i,j+1}-2\bar{p}_{0i,j}+\bar{p}_{0i,j-1}\right]$$

Substituting these expressions into the steady-state and perturbed Reynolds equations (3.3) and (3.4), we get

$$\bar{p}_{0i,j}=c_1\bar{p}_{0i+1,j}+c_2\bar{p}_{0i-1,j}+c_3\bar{p}_{0i,j+1}+c_4\bar{p}_{0i,j-1}+c_5 \tag{3.9}$$

$$\bar{p}_{1rpi,j}=c_1\bar{p}_{1rpi+1,j}+c_2\bar{p}_{1rpi-1,j}+c_3\bar{p}_{1rpi,j+1}+c_4\bar{p}_{1rpi,j-1} \tag{3.10}$$
$$+c_6\bar{p}_{0i+1,j}+c_7\bar{p}_{0i-1,j}+c_8\bar{p}_{0i,j+1}+c_9\bar{p}_{0i,j-1}+c_{10}\bar{p}_{0i,j}$$

$$\bar{p}_{1ipi,j}=c_1\bar{p}_{1ipi+1,j}+c_2\bar{p}_{1ipi-1,j}+c_3\bar{p}_{1ipi,j+1}+c_4\bar{p}_{1ipi,j-1}+c_{11} \tag{3.11}$$

where the perturbed film pressure has been expressed in terms of real and imaginary parts, $\bar{p}_1=\bar{p}_{1rp}+i\bar{p}_{1ip}$.

The coefficients c_0 to c_{11} are defined as

$$c_1=\delta^2b^2\left(\bar{f}_{0i+\frac{1}{2},j}+\frac{12\,\psi}{1-\beta}\right)/c_0$$

$$c_2=\delta^2b^2\left(\bar{f}_{0i-\frac{1}{2},j}+\frac{12\,\psi}{1-\beta}\right)/c_0\ ,\ c_3=c_4=\left(\bar{f}_{0i,j}+\frac{12\,\psi}{1-\beta}\right)/c_0\ ,$$

$$c_5=6\delta^2\lambda\left(\Delta\bar{z}\right)^2/c_0\ ,\ \ c_6=\delta^2b^2\bar{f}_{1i+\frac{1}{2},j}/c_0\ ,$$

$$c_7=\delta^2b^2\bar{f}_{1i-\frac{1}{2},j}/c_0\ ,\ c_8=c_9=\delta^2b^2\bar{f}_{1,j}/c_0\,,$$

$$c_{10}=-12\delta^2\lambda\left(\Delta\bar{z}\right)^2/c_0\,,$$

$$c_{11}=\left[\delta^2b^2\left(\bar{f}_{1i+\frac{1}{2},j}+\bar{f}_{1i-\frac{1}{2},j}\right)+2\bar{f}_{1i,j}\right]/c_0$$

$$c_0=\delta^2b^2\left(\bar{f}_{0i+\frac{1}{2},j}+\frac{12\,\psi}{1\text{-}\beta}+\bar{f}_{0i-\frac{1}{2},j}+\frac{12\,\psi}{1\text{-}\beta}\right)+2\left(\bar{f}_{0i,j}+\frac{12\,\psi}{1\text{-}\beta}\right) \tag{3.12}$$

and $b=\Delta\bar{z}/\Delta\bar{x}$.

The steady-state pressure and perturbed pressure are then calculated by using numerical method with grid spacing $\Delta\bar{x}=\Delta\bar{z}=0.05$

The steady-state load capacity W_s and perturbed film force W_d are evaluated by integrating the steady-state film pressure and perturbed film pressure respectively over the film region.

$$W_s=\frac{\mu UL^2B}{h_{m0}^2}\int_{x=0}^{x=L}\int_{z=0}^{z=B}p_0dx.dz\,, \tag{3.13a}$$

$$W_d=\frac{\mu UL^2B}{h_{m0}^2}\int_{x=0}^{x=L}\int_{z=0}^{z=B}p_1dx.dz\,. \tag{3.13b}$$

which in non-dimensional form

$$\bar{W}_s=\frac{W_sh_{m0}^2}{\mu UL^2B}=\int_{\bar{x}=0}^{\bar{x}=1}\int_{\bar{z}=0}^{\bar{z}=1}\bar{p}_0\ d\bar{x}.d\bar{z}\,, \tag{3.14a}$$
$$\approx\sum_{i=0}^{M}\sum_{j=0}^{N}\bar{p}_{0i,j}\Delta\bar{x}.\Delta\bar{z}$$

$$\bar{W}_d=\frac{W_dh_{m0}^2}{\mu UL^2B}=\int_{\bar{x}=0}^{\bar{x}=1}\int_{\bar{z}=0}^{\bar{z}=1}\bar{p}_1\ d\bar{x}.d\bar{z} \tag{3.14b}$$
$$\approx\sum_{i=0}^{M}\sum_{j=0}^{N}\bar{p}_{1i,j}\Delta\bar{x}.\Delta\bar{z}$$

where M+1 and N+1 are the grid-point numbers in the $\bar{x}-and\ \bar{z}$- directions respectively.

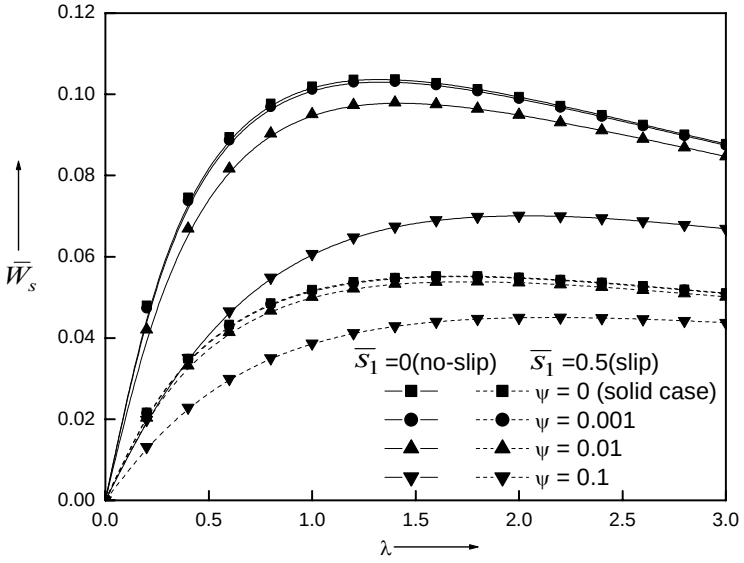

Fig.8 Variation of non-dimensional steady load-carrying capacity $\bar{W}_s$ with profile parameter λ for δ = 1.5, $\bar{l}$ = 0.1, β= 0.3

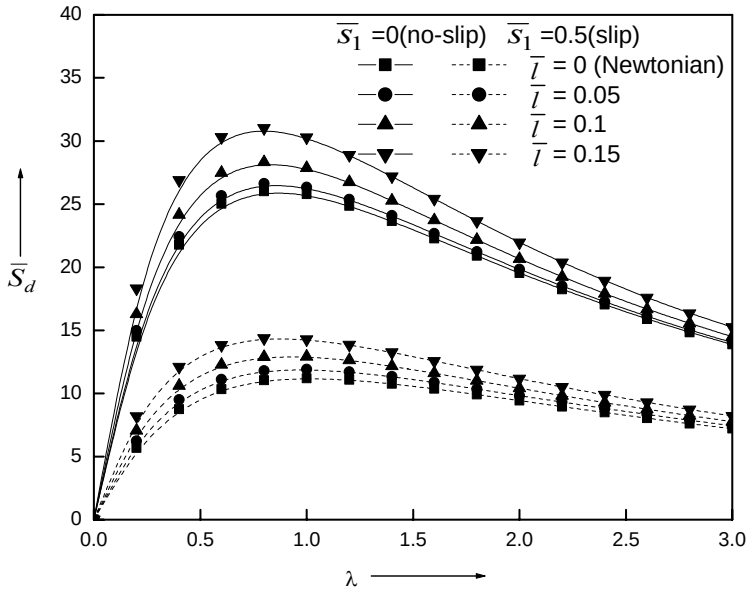

Fig.9 Variation of non-dimensional dynamic stiffness coefficient $\bar{S}_d$ with profile parameter λ for δ = 1.5, ψ = 0.01, β = 0.3

From the linear theory, the resulting dynamic film force can be expressed in terms of linearzed spring and damping coefficients.

$$W_d \varepsilon e^{i\bar{t}} = -S_d h_{m0} \varepsilon e^{i\bar{t}} - C_d \frac{d}{dt}(h_{m0} \varepsilon e^{i\bar{t}}) . \qquad (3.15)$$

which in non-dimensional form

$$\bar{W}_d = -\bar{S}_d - i\bar{C}_d \qquad (3.16)$$

where

$$\bar{S}_d = \frac{S_d h_{m0}^3}{\mu U L^2 B} \quad and \quad \bar{C}_d = \frac{C_d h_{m0}^3}{\mu L^3 B} .$$

The dimensionless stiffness coefficient $\bar{S}_d$ and the damping coefficient $\bar{C}_d$ are obtained by equating the real and imaginary parts of $\bar{W}_d$ respectively as

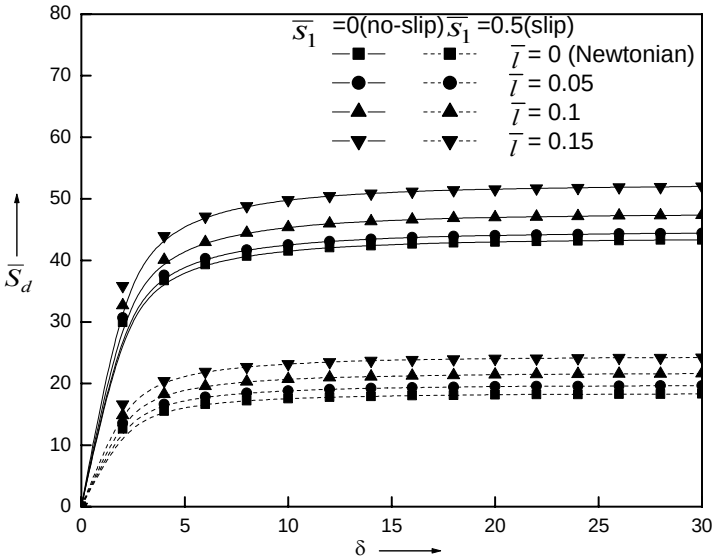

Fig.10 Variation of non-dimensional dynamic stiffness coefficient $\overline{S}_d$ with aspect ratio δ for λ =0.75 ψ = 0.01, β= 0.3

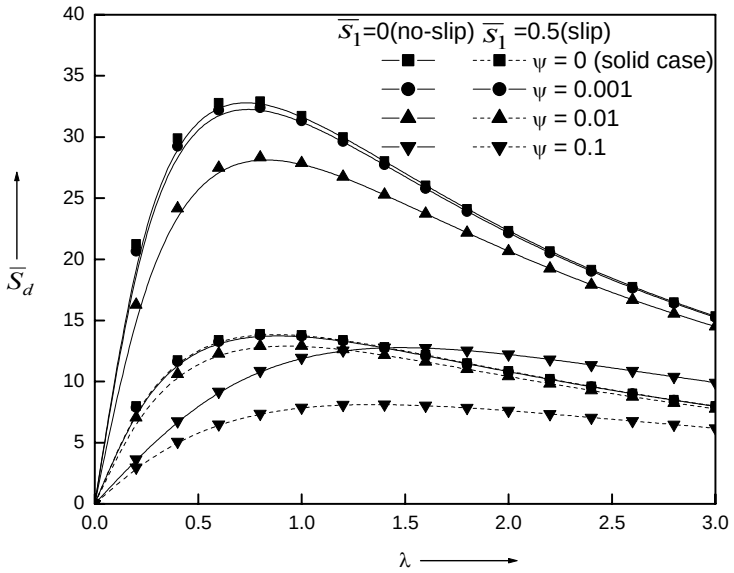

Fig.11 Variation of non-dimensional dynamic stiffness coefficient $\overline{S}_d$ with profile parameter λ for δ = 1.5, $\overline{l}$ = 0.1, β= 0.3

$$\overline{S}_d = -\mathrm{Re}(\overline{W}_d) \approx -\sum_{i=0}^{M}\sum_{j=0}^{N}\left(\overline{p}_{1rp}\right)_{i,j}\Delta\overline{x}.\Delta\overline{z}\,, \qquad (3.17a)$$

$$\overline{C}_d = -\mathrm{Im}(\overline{W}_d) \approx -\sum_{i=0}^{M}\sum_{j=0}^{N}\left(\overline{p}_{1ip}\right)_{i,j}\Delta\overline{x}.\Delta\overline{z} \qquad (3.17b)$$

RESULTS AND DISCUSSION

To solve the steady-state and perturbed film pressures in the equations (3.9), (3.10) and (3.11) the mesh for the domain has 20 equal intervals along length and breadth. The coefficient matrix of the system of algebraic equations is of pentadiagonal form. These equations have been solved by using SciLab tools.

According to Stokes micro-continuum theory the new material parameter η in the Eqn. (1.1) is responsible for the property of couple stresses. Since the dimension of $l\left(=\sqrt{\frac{\eta}{\mu}}\right)$ is of length, it can be regarded as the chain length

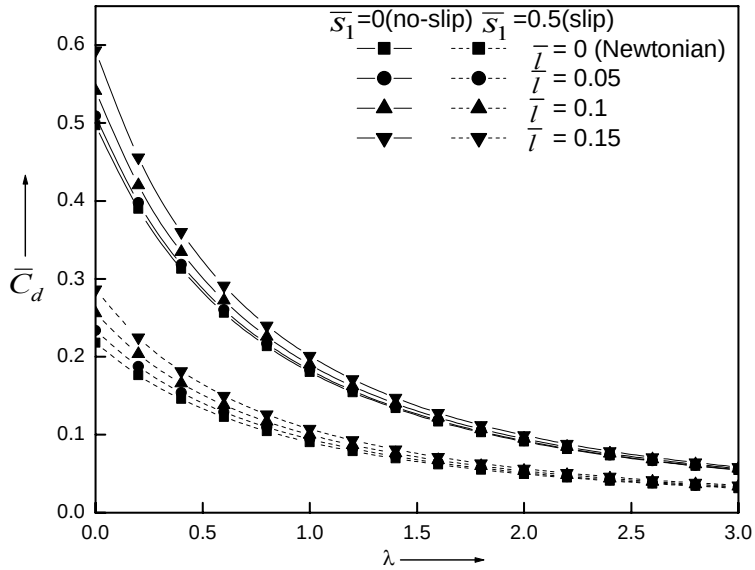

Fig.12_Variation of non-dimensional dynamic damping coefficient $\overline{C}_d$ with profile parameter λ for δ = 1.5, ψ = 0.01, β = 0.3

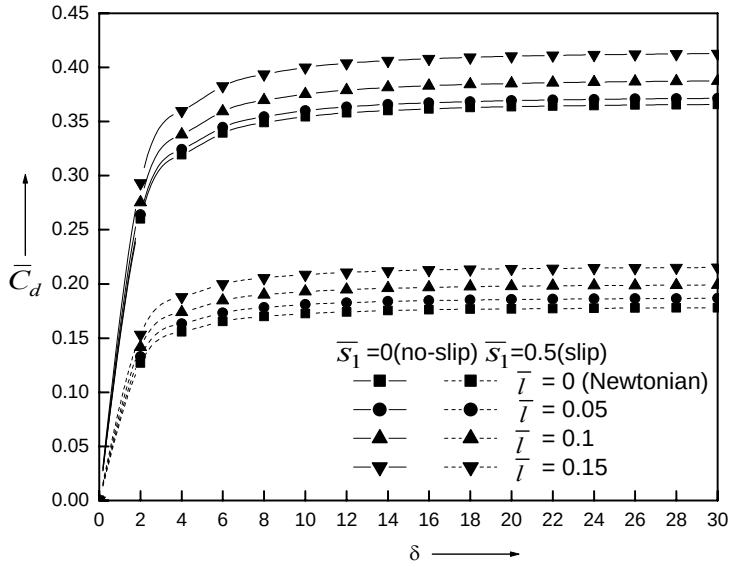

Fig.13. Variation of non-dimensional dynamic damping coefficient Cd* $\overline{C}_d$ with aspect ratio δ for λ = 0.75 for β = 0.3 and ψ=0.01

of microstructure additives present in the lubricant. Therefore, the non dimensional couple stress parameter $\overline{l}\left(=\frac{l}{h_{m0}}\right)$ provides the mechanism of interaction of the fluid with the bearing geometry.

It is expected that the couple stress effects are prominent either when the molecular size of additives is large or the minimum film thickness is small. *i.e.* when $\overline{l}$ is large. The numerical values of $\overline{l}$ should be less than 1 for the validity of hydrodynamic lubrication *i.e.* the size of polar additives must be less than the minimum film thickness. In this paper, with the aid of the non-dimensional parameter $\overline{l}$, the effect of the couple stresses upon the steady-state performance and dynamic characteristics of infinitely wide inclined porous slider bearings is studied. The effect of the permeability on the static and dynamic

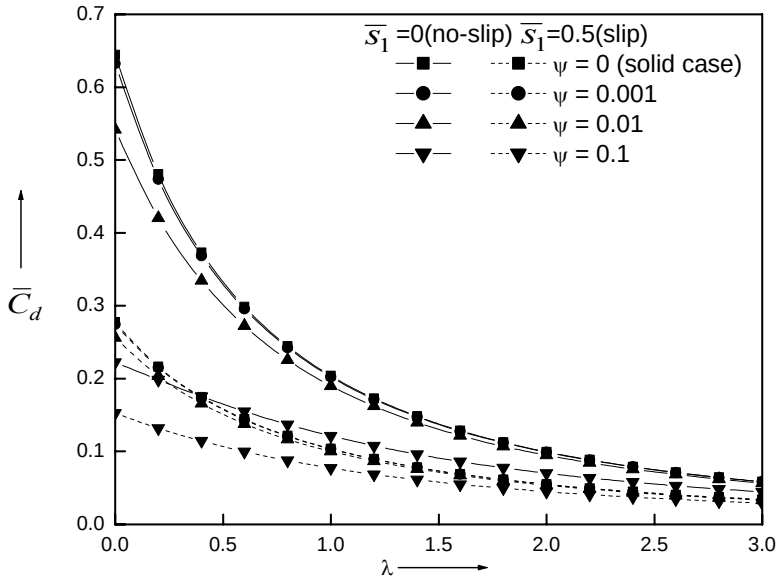

Fig.14 Variation of non-dimensional dynamic damping coefficient $\overline{C}_d$ with profile parameter λ for δ = 1.5, $\overline{\iota}$ = 0.1, β= 0.3

characteristics of the bearings is analyzed through the permeability parameter $\left(\psi = \frac{k\delta}{h_{m0}^3}\right)$ and the effect of the slip is characterized by the slip parameter $\overline{s}_1$. In the limiting case $\psi \to 0 \quad and\ \overline{s}_1 \to 0$, the modified Reynolds equation (2.23) reduces to the solid case studied by Lin *et al*. (2003).

The variation of non-dimensional steady-state pressure P_0 for different values of couple stress parameter $\overline{l}$ is depicted in the Fig.. 4. It is observed that P_0 increases for increasing values of $\overline{l}$. The effect of permeability parameter ψ on the variation of P_0 is depicted in the Fig.5. for the aspect ratio $\delta = 1.5$. It is observed that P_0 decreases for increasing values of ψ.

The variation of non-dimensional steady-load carrying capacity $\overline{W}_s$ with the profile parameter λ is depicted in Fig.6 for different values of the couples tress parameter $\overline{l}$ with $\beta = 0.3$, $\delta = 1.5$ and $\psi = 0.01$ for both slip ($\overline{s}_1$=0.5) and no slip ($\overline{s}_1$=0) cases. It is observed that, the effect of couple stresses is to increase $\overline{W}_s$ as compared to the corresponding Newtonian case ($\overline{l}$ = 0). Further it is also observed that the effect of slip on the porous interface reduces $\overline{W}_s$ significantly as compared to the no slip case ($\overline{s}_1$=0). The effect of velocity slip is to decrease the resistance encountered by the lubricants flow in the fluid film gap this leads to the reduction in the load carrying capacity $\overline{W}_s$. The stronger slip (larger values of $\overline{s}_1$) decreases the resistance of lubricant flow with an extent that there is a lesser tendency for lubricant to flow through the porous material. It is interesting to note that the existence of the critical value λ_c for the profile parameter λ at which the steady-load carrying capacity attains maximum. Eg, for $\overline{l}$ = 0.1 and ψ=0.01. λ_c=1.4 for no slip case and λ_c=1.8 for the slip case. Fig.7 depicts the variation of $\overline{W}_s$ with aspect ratio δ for various values of the couple stress parameter $\overline{l}$ with $\lambda = 0.75$, $\beta = 0.3$ and $\psi = 0.01$. The rapid increase in $\overline{W}_s$ is observed for smaller values of δ however the increase in $\overline{W}_s$ is marginal for larger values of δ (δ>5.0). Further it is observed that the couple stress fluid provides an increased non-dimensional steady load carrying capacity as compared to the Newtonian case ($\overline{l}$ =0).

Fig.8 depicts the variation of non-dimensional steady-load carrying capacity $\overline{W}_s$ with λ for different values of

permeability parameter ψ for both slip ($\bar{s}_1$=0.5) and no slip ($\bar{s}_1$=0) cases. It is observed that, the effect of ψ is to decrease the value of $\bar{W}_s$ for both slip and no slip cases. When the permeability is very high (larger values of ψ) the porous material becomes the main path of flow and hence decreases $\bar{W}_s$. Further it is observed that the critical value of λ, λ_c is a function of the permeability parameter, ψ. λ_c increases for increasing values of ψ.

Fig. 9 depicts the variation of non-dimensional dynamic stiffness coefficient $\bar{S}_d$ with profile parameter λ for various values of the couple stress parameter $\bar{l}$ for both slip ($\bar{s}_1$= 0.5) and no slip ($\bar{s}_1$= 0) cases. It is observed that, the effect of couple stresses is to increase $\bar{S}_d$ as compared to the corresponding Newtonian case ($\bar{l}$ = 0). It is also observed that, the effect of slip on the porous interface reduces $\bar{S}_d$ significantly as compared to the no slip case. Further it is observed that at the critical value of λ, the non-dimensional dynamic stiffness coefficient attains the maximum value. The variation of $\bar{S}_d$ with δ for various values of couple stress parameter $\bar{l}$ is shown in Fig.. 10 for both slip and no slip cases. The sharp increase in $\bar{S}_d$ is observed for smaller values of the aspect ratio δ ($0<\delta<5$) and the increase in $\bar{S}_d$ is marginal for larger values of δ. The variation of $\bar{S}_d$ with λ for different values of the permeability parameter ψ for both slip and no slip cases is shown in the Fig.11. It is observed that as permeability parameter ψ increases, the value of $\bar{S}_d$ decreases. Similar trend is observed for no slip case.

Fig. 12 displays the variation of non-dimensional dynamic damping coefficient $\bar{C}_d$ with profile parameter λ for various values of $\bar{l}$ with β=0.3. It is observed that the effect of couple stresses on the dynamic damping coefficient is marginal for the larger values of λ. But there is a significant increase in the value of $\bar{C}_d$ for the bearing under a smaller profile parameter. It is also observed that the significant reduction in the value of $\bar{C}_d$ for the slip case ($\bar{s}_1$= 0.5) as compared to the no slip case ($\bar{s}_1$= 0). The variation of non-dimensional dynamic damping coefficient $\bar{C}_d$ with aspect ratio δ for various values of $\bar{l}$ with ψ=0.01, $\lambda = 0.75$ and β=0.3. It is observed that $\bar{C}_d$ increases rapidly for smaller values of δ ($0<\delta<4$) however marginal increase is observed in $\bar{C}_d$ for larger values of δ. Further, it is observed that the effect of couple stresses is to increase $\bar{C}_d$ as compared to the corresponding Newtonian case.

Fig. 14 depicts the variation of non-dimensional dynamic damping coefficient $\bar{C}_d$ with profile parameter λ for the values of permeability parameter ψ with $\bar{l}$=0.1 and β=0.3. It is observed that, the increase in the profile parameter λ decreases the value of $\bar{C}_d$ and similar trend is observed for the no slip case. The larger values of the profile parameter λ (λ>2.0) have marginal effect on the variations of the dynamic damping coefficient, $\bar{C}_d$.

CONCLUSIONS

The general Reynolds type equation for the porous slider bearings with squeezing effects is derived for the couple stress fluids on the basis of Stokes micro-continuum theory for the couple stress fluids by using the modified B-J-slip boundary conditions on the fluid-porous interface. The numerical results are obtained for the finite porous inclined slider bearings. On the basis of the results presented, the following conclusions are drawn:

1. The critical value of the profile parameter λ, λ_c exists such that the steady-state load carrying capacity $\bar{W}_s$, the dynamic stiffness coefficient $\bar{S}_d$ attains maximum at λ_c
2. The critical value of the profile parameter λ_c is a function of the permeability parameter ψ and this dependence is more pronounced for the no slip case.
3. The presence of porous facing on the slider decreases the $\bar{W}_s$, $\bar{S}_d$ and $\bar{C}_d$
4. The couple stress fluid lubricants provide an increased steady-load carrying capacity, dynamic stiffness and decreases the dynamic damping coefficient. These effects are more pronounced for larger values of the aspect ratio.

ACKNOWLEDGEMENTS

The authors sincerely acknowledge the financial assistance by UGC New Delhi, INDIA under major research project No.F31-84/2005(SR). And one of the

authors (GBM) thankful to Dr. Ashok S. Shettar, Principal, B.V.B.College of Engineering and technology, Hubli-31 for his encouragements.

REFERENCES

Akhverdiev, KS., Prikhodko, VM., Shevchenko, AI. and Kazanchyan, OP. 2000. Hydrodynamic analysis of heterogeneous three- layered porous bearings with variable permeability along the axis. Jl. Friction and Wear 21. (4): 23-29.

Ariman, T., Turk, MA. and Sylvester, ND.1973. Micro-continuum fluid mechanics – a Review. Int. J. Eng. Sci. 11:905-930.

Ariman, T., Turk, MA. and Sylvester, ND.1974. Applications of micro-continuum fluid mechanics. Int. J. Eng. Sci. 12: 273-293.

Bujurke, NM., Naduvinamani, NB. and Benchalli, SS. 2005. Secant shaped porous Slider bearing lubricated with couple stress fluids. Ind. Lub. and Technol. 57:155-160.

Gupta, RS. and Kapur, VK. 1979. Centrifugal effects in hydrostatic porous thrust Bearings. J. Lub. Tech. 101:381-392.

Kumar, V. 1980. Friction of a plane porous slider of optimal profile. Wear 62: 417-418.

Lahmar, M. 2005. Elastohydrodynamic analysis of double layered journal bearings with couple stress fluids. Proc. Inst. Mech. Engrs. Part J. 219:145-171.

Lin, JR., Lu, Rf. and Chang, TB. 2003. Derivation of dynamic couple stress Reynolds equation of sliding squeezing surfaces and numerical solution of plane inclined slider bearing. Trib.Int. 36: 679-685.

Morgan, VT. and Cameron, A. 1957. Mechanism of lubrication in porous metal Bearings. Proc. of Conf. on Lubrication and Wear. Institute of Mechanical Engineers. London. 151-157.

Murti, PRK. 1974a. Analysis of porous slider bearings. Wear 28:131-134.

Murti, PRK. 1974b. Squeeze-film behaviors in porous circular disks. ASME J. Lub. 96: 206-219.

Naduvinamani, NB., Hiremath, PS. and Gurubasawaraj, G. 2001a. Squeeze film lubrication of a short porous journal bearing with couple stress fluids. Trib. Intnl.34: 739-747.

Naduvinamani, NB., Hiremath, PS. and Syeda Tasneem Fathima. 2002. Lubrication of a narrow porous journal bearing with a couple stress fluid. Lub Sci. 14(4) :393-413.

Naduvinamani, NB., Hiremath, PS. and Syeda Tasneem Fathima. 2004. On the squeeze effect of lubricants with additives between rough porous rectangular plates. ZAMM 84.12:825-834.

Naduvinamani, NB., Hiremath, PS. and Gurubasawaraj, G. 2001b. Static and dynamic bearing of squeezing film lubrication of narrow porous journal bearings with couple stress fluid. Proc Instn Mech Engrs. 215J:45-62.

Pinkus, O. and Sternlicht, B. 1961. Theory of hydrodynamic lubrication. New York: McGraw-Hill.
Prakash, J. and Vij, SK. 1974. Squeeze films in porous bearings. Wear. 7:359-366.

Ramanaiah, G. and Priti Sarkar. 1978. Squeeze films and thrust bearings lubricated by fluids with couple stress. Wear. 48:309-316.

Ramanaiah, G. 1979. Squeeze films between finite plates lubricated by fluids with couple Stress. Wear. 54 : 315-320.

Robin, M. 1978. Etude de la lubrication des paliers de longuer finie: Influence des additives. De viscosity, the de doctorate. Edition technip.

Sanni, SA. and Ayomidele, IO. 1991. Hydrodynamic lubrication of a porous slider: limitation of the simplifying assumption of a small porous facing thickness. Wear. 147: 1-7.

Srinivasan, U. 1977. The analysis of a double layered porous slider bearing. Wear. 42: 205- 215.

Stokes, VK. 1966. Couple stresses in fluids. The physics of fluids 9: 1709-1715.

Uma, S. 1977. The analysis of double-layered porous slider bearing. Wear. 42: 205-215.

Verma, PDS., Agrawal, V K. and Bhatt, SB. 1978. The optimum profile for a porous slider Bearing. Wear. 48: 9-14.

Wu, H. 1972. An analysis of the squeeze film between porous rectangular plates. ASME Jl. Lub. Technol. 94: 64-68.

NOMENCLATURE

a difference between inlet and outlet film thickness
B width of the bearing
C_d damping coefficient,

$\bar{C}_d$ non-dimensional damping coefficient $\left(=\frac{C_d h_{m0}^3}{\mu L^3 B}\right)$

h film thickness function
h_m minimum film thickness at the outlet
h_s slider profile function
h_{m0} steady-state minimum film thickness at the outlet
k permeability of the porous material
l couple stress parameter
$\bar{l}$ non-dimensional couple stress parameter $\left(=\frac{l}{h_{m0}}\right)$

L length of the bearing
p dynamic film pressure
$\bar{p}$ non-dimensional dynamic film pressure $\left(=\frac{ph_{m0}^2}{\mu UL}\right)$

p^* pressure in the porous region

p_0 steady film pressure

$\bar{p}_0$ non-dimensional steady film pressure $\left(=\frac{p_0 h_{m0}^2}{\mu UL}\right)$

p_1 perturbed film pressure

$\bar{p}_1$ non-dimensional perturbed film pressure $\left(=\frac{p_1 h_{m0}^2}{\mu UL}\right)$

δ aspect ratio (=B/L)
s slip parameter $\left(=\frac{\alpha}{\sqrt{k}}\right)$

S_d stiffness coefficient,
$\bar{S}_d$ non-dimensional stiffness coefficient $\left(=\frac{S_d h_{m0}^3}{\mu UL^2 B}\right)$

t time
u, v, w velocity components
U sliding velocity of the lower part
W_s steady load carrying capacity,
$\bar{W}_s$ non-dimensional steady load carrying capacity $\left(=\frac{W_s h_{m0}^2}{\mu UL^2 B}\right)$

W_d perturbed film force,
$\bar{W}_d$ non-dimensional perturbed film force $\left(=\frac{W_d h_{m0}^2}{\mu UL^2 B}\right)$

x, y, z Cartesian rectangular coordinates
β ratio of microstructure size to the pore size $\left(=(\eta/\mu)/k\right)$
ε small amplitude of oscillation
η material constant responsible for the couple stress property
ρ lubricant density
∇ gradient operator

λ non-dimensional profile parameter of the bearing $\left(=\frac{a}{h_{m0}}\right)$
μ classical viscosity coefficient
ψ permeability parameter $\left(=\frac{kH}{h_{m0}^3}\right)$

$\frac{D}{Dt}$ material derivative